

ICONN 2015 [4<sup>th</sup> -6<sup>th</sup> Feb 2015]

International Conference on Nanoscience and Nanotechnology-2015

SRM University, Chennai, India

## Electrodeposition of Cerium Substituted Hydroxyapatite Coating on Passivated Surgical Grade Stainless Steel for Biomedical Application

S. Sathishkumar<sup>1,2\*</sup>, A. Karthika<sup>1</sup>, M.Surendiran<sup>1</sup>,  
L. Kavitha<sup>3</sup> and D. Gopi<sup>1,2</sup>

<sup>1</sup>Department of Chemistry, Periyar University, Salem 636 011, Tamilnadu, India

<sup>2</sup>Centre for Nano science and Nanotechnology, Periyar University,  
Salem 636 011, Tamilnadu, India

<sup>3</sup>Department of Physics, School of Basic and Applied Sciences, Central University of  
Tamilnadu, Thiruvavur-610 101, Tamilnadu, India

**Abstract :** Surgical grade stainless steel (316L SS) is mostly used in orthopedic implants due to its good mechanical properties, corrosion resistance and good biocompatibility. Though it possesses advantages, the surface of stainless steel is prone to release metal ions in the physiological medium. For this reason, it is important to introduce bioceramic coatings on the metallic surface to improve the biocompatibility and corrosion resistance. The present work is dealt with successful development of cerium substituted hydroxyapatite (Ce-HAP) on borate passivated 316L SS. The coatings were characterized by Fourier transform infrared spectroscopy (FT-IR), X-ray diffraction (XRD), scanning electron microscopy (SEM) and energy dispersive X-ray analysis (EDAX). The electrochemical characterization such as using potentiodynamic cyclic polarization and electrochemical impedance spectroscopic techniques of Ce-HAP coating on the passivated 316L SS in Ringer's solution demonstrated the enhanced anti-corrosion performance of Ce-HAP coating. The antimicrobial performance was studied for the obtained coatings against the pathogenic bacterial strains *S. aureus* and *E. coli*. Thus, the Ce-HAP coating on the passivated 316L SS can play a significant role in the biomedical applications.

**Key words:** 316L SS, passivation, substituted hydroxyapatite, corrosion resistance, antibacterial activity.

### 1. Introduction

Austenitic stainless steels are widely used as orthopedic implants due to the advantages such as low cost, excellent processability, ease of fabrication, good mechanical properties linked to bone mineral<sup>1</sup>. The metal surface of stainless steel is prone to release chromium, iron and nickel ions in human body<sup>2</sup>. The leached chromium and nickel ions are toxic species and powerful allergens and to be carcinogenic. In order to protect the metal ion release, the bioactive ceramic coatings especially hydroxyapatite [Ca<sub>10</sub>(PO<sub>4</sub>)<sub>6</sub>(OH)<sub>2</sub>, HAP] was

developed on the surface of the implant material<sup>3,4</sup>. During the past decades, HAP has been a subject of serious research due to its chemical similarity to the mineral components of bones and tissues in mammals. The properties of HAP were specified to be controlled by its crystal structure and composition. Consequently the substitution of  $\text{Ca}^{2+}$  with other metal ions plays a vital role in the improvement of biological performance of HAP<sup>5</sup>. Cerium ion belongs to lanthanide group, which can play a significant role in preventing caries. However, only few studies have dealt with Ce-HAP for antibacterial activity<sup>6,7</sup>. The  $\text{Ce}^{3+}$  substituted HAP results in the increase of solubility, which may sequentially developed in the biodegradability and antibacterial activity<sup>8,9</sup>.

However, due to the continuous interaction with the harsh environment, the HAP or substituted HAP on the metallic surface degrades as the time progress and results in the corrosion of metallic alloy. Hence surface treatment of metal alloy prior to the development of coating is essential in the prevention of metallic corrosion and to with stand during the long term implant conditions<sup>10, 11</sup>. have achieved the successful borate passivation on the SS surface and studied the effect of the HAP coating on it by electrodeposition method. In the present work, we have reported the successful electrodeposition of Ce-HAP coating on borate passivated 316L SS. The coating was characterized by Fourier transform infrared spectroscopy (FT-IR), X-ray diffractometry (XRD), scanning electron microscopy (SEM) and energy dispersive X-ray analysis (EDAX) techniques. The corrosion behavior of the resultant coating was evaluated using potentiodynamic cyclic polarization technique as well as electrochemical impedance spectroscopy in Ringer's solution. In addition, the antimicrobial property of the Ce-HAP on borate passivated 316L SS was tested against *Staphylococcus aureus* (*S. aureus*) and *Escherichia coli* (*E. coli*) strains. The Ce-HAP coating on borate passivated 316L SS will serve as a promising candidate with improved corrosion resistance and antibacterial property.

## 2. Experimental

### 2.1 Substrate preparation

The 316L SS (procured from Steel Authority of India Ltd., (SAIL), India) having elemental composition (wt%) C-0.0222, Si-0.551, Mn-1.67, P-0.023, S-0.0045, Cr-17.05, Ni-11.65, Mo-2.53, Co-0.136, Cu-0.231, Ti-0.0052, V-0.0783, N-0.0659 and rest Fe were cut into dimensions of  $10 \times 10 \times 3$  mm. These substrates were embedded with epoxy resin leaving area of  $1 \text{ cm}^2$  for exposure to the electrolyte. Prior to the deposition process, all the substrates were abraded with silicon carbide sheets from 400 to 1200 grits. After polishing, the 316L SS substrates were thoroughly washed with deionized (DI) water and ultrasonically cleaned in acetone for 10 min, and then used for further studies.

### 2.2 Borate passivated of 316L SS

The 316L SS were potentiostatically held in 0.4 M borate buffer solution (pH 9.3) at 640 mV vs SCE for 1 h. An anodic potential of 640 mV vs SCE was applied after which the electrode was gradually rinsed in acetone and double distilled water and immediately transferred to the analyzing chamber. Electrochemical deposition of Ce-HAP was carried out on these passivated substrates according to the following procedure.

### 2.3 Preparation of electrolyte

The electrolyte for the deposition was prepared by dissolving analytical grade  $\text{Ca}(\text{NO}_3)_2 \cdot 6\text{H}_2\text{O}$  (0.45 M) and  $\text{Ce}(\text{NO}_3)_3 \cdot 6\text{H}_2\text{O}$  (0.05 M) were dissolved separately in DI water. The  $(\text{NH}_4)_2\text{HPO}_4$  (0.3 M) was dissolved in DI water and the solutions were mixed in the molar ratio of 1.67. The electrolyte was kept in a magnetic stirrer for 2 h and the pH of the electrolyte was adjusted at 4.5 by using  $\text{NH}_4\text{OH}$  solution.

### 2.4 Electrochemical deposition on 316L SS

The resultant solution was used as electrolyte for the electrochemical deposition process where the pristine and passivated 316L SS substrates served as cathode, platinum electrode acted as anode and the saturated calomel electrode (SCE) acted as reference electrode. Constant cathodic potential of -1400 mV vs SCE were applied by means of electrochemical workstation (CHI 760C, CH instruments, USA) for the duration of 1 h in the potentiostatic mode. The temperature during the deposition was maintained at  $50^\circ\text{C}$  and the pH was maintained at 4.5. After the electrodeposition, the as-coated substrates were gently rinsed in deionized water and used for further studies.

## 2.5 Surface characterizations of resultant coatings

The functional groups of the coatings was characterized by Fourier transform infrared spectroscopy (Perkin Elmer RX1 Spectrometer), in the over frequency recorded in the range  $4000$  to  $400\text{ cm}^{-1}$ . The phase compositions of the coatings were identified by X-ray diffraction (XRD) PANalyticalX'Pert PRO diffractometer in the range between  $20^\circ \leq 2\theta \leq 70^\circ$  with Cu  $K\alpha$  radiation ( $1.5406\text{ \AA}$ ). The surface morphology and actual composition of the coating were observed using high resolution scanning electron microscopy (HRSEM, JSM 840A, JEOL-Japan) equipped with EDAX.

## 2.6 Antibacterial studies

The gram positive *S. aureus* and negative bacterial strains *E. coli* were used to study the antibacterial activity of the Ce-HAP coating by the agar disc diffusion method. The inoculums of the microorganisms were prepared from fresh overnight broth cultures that were incubated at  $37 \pm 1^\circ\text{C}$ . The agar disc diffusion test was performed at Muller-Hinton agar. The diffusion method was carried out by pouring agar into petri dish to form  $4\text{ mm}$  thick layers and adding dense inoculums of the tested microorganisms in order to obtain semi confluent growth. Petri dishes were left for  $10\text{ min}$  to dry in the air and after that, discs were prepared from Whatmann filter paper and immersed in different concentrations of the as developed coating such as  $25\mu\text{l}$ ,  $50\mu\text{l}$ ,  $75\mu\text{l}$  and  $100\mu\text{l}$  and then the discs were placed at equal distance and incubated for  $24\text{ h}$  at  $37^\circ\text{C}$ .

## 3. Results and discussion

### 3.1 FT-IR analysis

Figure 1 shows the FT-IR spectrum of the Ce-HAP coating and the characteristic peaks found at  $475$ ,  $590$ ,  $604$ ,  $952$ , and  $1031\text{ cm}^{-1}$  depicted to the phosphate groups. The bands at  $3447\text{ cm}^{-1}$  and  $1623\text{ cm}^{-1}$  are attributed to the stretching and bending mode of water molecule. The absorption bands at  $3582\text{ cm}^{-1}$  and  $632\text{ cm}^{-1}$  are assigned to the stretching and bending vibration of  $\text{OH}^-$  groups of Ce-HAP. All the peaks confirm the formation of Ce-HAP coating, but some changes in IR wavenumber of bands observed due to the substitution of  $\text{Ca}^{2+}$  by  $\text{Ce}^{3+}$  into the apatite lattice where the ionic radius of  $\text{Ca}^{2+}$  is  $0.100\text{ nm}$  and  $\text{Ce}^{3+}$  is  $0.107\text{ nm}$ . The higher radius of  $\text{Ce}^{3+}$  consequently decreases the bonding strength of P-O and OH group.

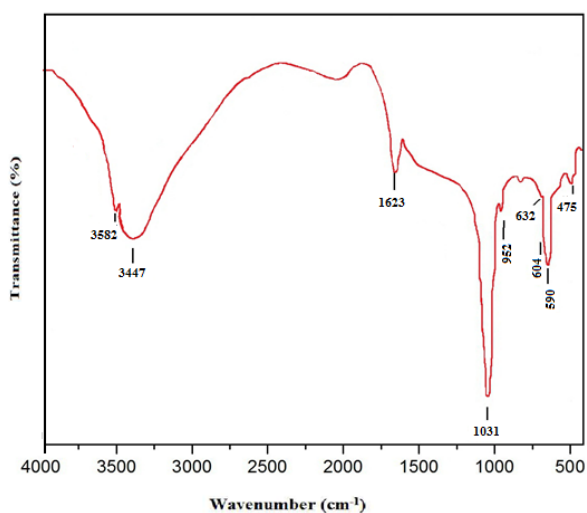


Fig. 1 The FT-IR spectrum of Ce-HAP coating at  $-1400\text{ V}$

### 3.2 X-ray diffraction studies

The XRD patterns of the Ce-HAP coating was displayed as Fig. 2. The main diffraction peaks of  $2\theta$  values of  $25.88^\circ$ ,  $31.77^\circ$ ,  $32.3^\circ$  and  $32.9^\circ$  was experienced a slight shift towards the lower diffraction angle which evidence the substitution of Ce ion in HAP lattice. This shift may occur due to the higher ionic radius of Ce ion ( $0.107\text{ nm}$ ) compared with Ca ( $0.100\text{ nm}$ ). All the peaks confirm the presence of HAP which are well evident from the ICDD card No: 09-0432. The intense diffraction peaks resembles the crystalline nature of the Ce-HAP coating as evidenced in the Fig. 2.

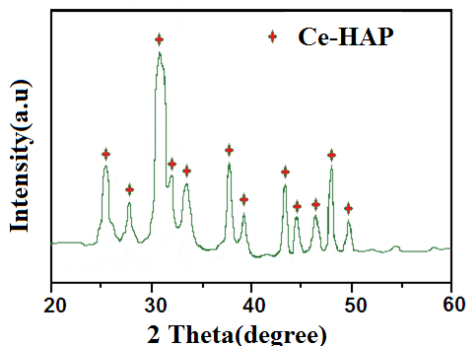


Fig. 2 The XRD pattern of Ce-HAP coating at -1400 V

### 3.3 SEM and EDAX analysis

Figure 3(a-c) shows the SEM microstructure of the borate passivated 316L SS, Ce-HAP coating on pristine 316L SS and Ce-HAP coating on passivated 316L SS. The Fig. 3(a) shows the passivated surface of the 316L SS without any pits and cracks. The Ce-HAP coating on pristine 316L SS exhibited non-uniform rod like structure as shown in Fig. 3(b). Moreover, the Ce-HAP coating on passivated 316L SS was fully covered with uniform rod like structure (Fig. 3(c)). The EDAX spectrum results indicate the presence of calcium (Ca), phosphorous (P), cerium (Ce), and oxygen (O) elements in the Ce-HAP.

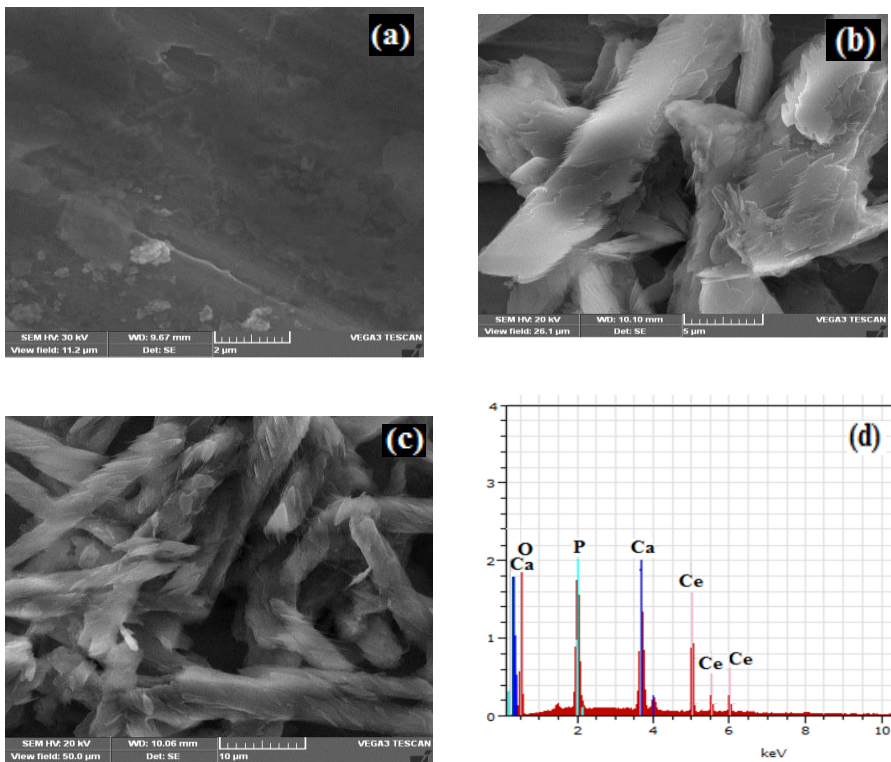
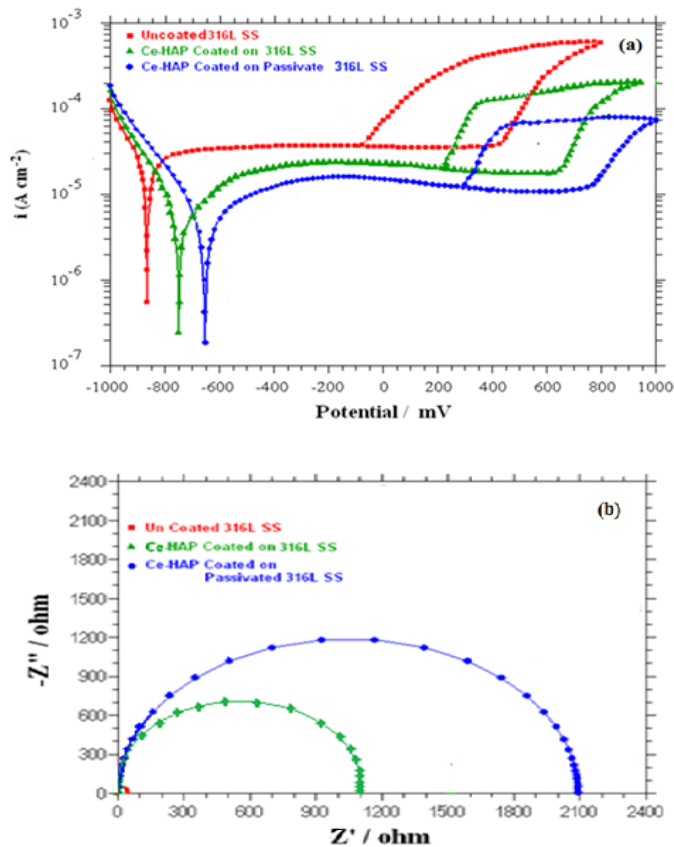


Fig. 3 SEM images of (a) passivated 316L SS (b) Ce-HAP coating on pristine 316L SS (c) Ce-HAP coating on passivated 316L SS and (d) EDAX spectrum of (c).

### 3.4 Electrochemical studies

The corrosion resistance of the uncoated 316L SS, Ce-HAP coating on pristine and passivated 316L SS was studied in Ringers solution. The corrosion potential ( $E_{\text{corr}}$ ), breakdown potential ( $E_b$ ) and repassivation potential ( $E_{\text{pp}}$ ) were calculated (Fig.4a) from the curve which is listed in Table 1.



**Fig. 4 Electrochemical studies of Ce-HAP coating (a) potentiodynamic polarization curve and (b) impedance curve.**

The Ce-HAP coating on passivated 316L SS specimens showed positive shift compared to the uncoated and other coatings. This positive shift values indicated the Ce-HAP coating on passivated 316L SS has excellent corrosion resistance in Ringer's solution. The Nyquist plots (Fig.4b) obtained for uncoated, Ce-HAP coating on pristine and passivated 316L SS were performed in Ringer's solution. The polarization resistance ( $R_p$ ) and the total impedance ( $|Z|$ ) values were listed in Table 1. The Ce-HAP coated on passivated 316L SS values higher than other coated samples. Hence, the excellent corrosion resistance behavior of the Ce-HAP coating was observed in Ringer's solution.

**Table 1 : Electrochemical parameters of uncoated SS, Ce-HAP on pristine and Ce-HAP coatings on borate passivated 316L SS**

S. No.	Samples	$E_{corr}$ (mV)	$E_b$ (mV)	$E_{pp}$ (mV)	$R_p$ ( $\Omega \text{ cm}^2$ )	$ Z $ ( $\text{cm}^2$ )
1	Uncoated pristine 316L SS	-870	+449	-90	41	58
2	Ce-HAP on 316L SS	-762	+641	+210	1102	1453
3	Ce-HAP on passivated 316L SS	-642	+776	+243	2086	2416

### 3.5 Antibacterial activity

The antibacterial activity of the Ce-HAP coating was tested against two bacterial strains *E.coli* and *S.aureus* at four different volumes such as 25, 50, 75 and 100  $\mu\text{l}$  (Fig. 5). The results demonstrated that the Ce-HAP coated samples increases the inhibition zone as increasing the concentration of samples. As shown in the figure, the inhibition zone for Ce-HAP at all concentration is higher for gram negative bacteria than gram positive bacteria, which explains the better sensitivity of resultant coating.

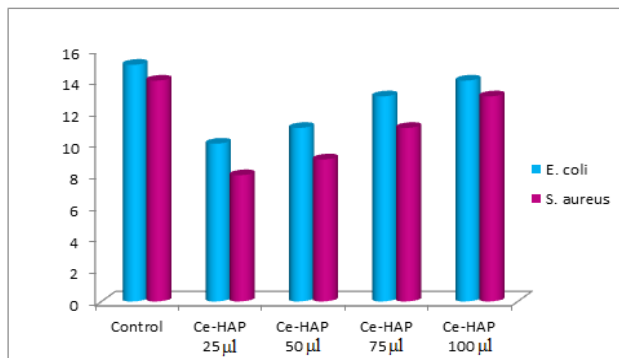


**Fig. 5 Antibacterial activity of Ce-HAP coating at different concentration against pathogenic bacteria *E.coli* and *S.aureus*.**

#### 4. Conclusion

The intension of authors is to develop the Ce-HAP coating on borate passivated 316L SS by the electrodeposition method. The XRD and FT-IR studies confirmed the high crystallinity and the functional groups of Ce-HAP coating. The morphological results revealed that the Ce-HAP coating achieved on passivated 316L SS with uniform coverage of rods. The corrosion resistance of the Ce-HAP coating exhibited appreciable protection in Ringer's solution. The excellent antibacterial activity was observed for the Ce-HAP coating. Hence the developed Ce-HAP coating can be served as potent material for biomedical applications.

#### References

1. Javidi, M., Javadpour, S., Bahrololoom, M. E., and Ma Electrophoretic deposition of natural hydroxyapatite on medical grade 316L stainless steel. *Materials Science and Engineering C*. 2008, 28; 1509-15.
2. Sivakumar, M., and Rajeswari, S., Investigation of failures in stainless steel orthopaedic implant devices: pit-induced stress corrosion cracking. *J. Mater. Sci. Lett.*, 1992, 11; 1039.
3. Gopi, D., Karthika, A., Nithiya, S., and Kavitha, L., In vitro biological performance of minerals substituted hydroxyapatite coating by pulsed electrodeposition method. *Mater. Chem. Phys.*, 2014, 144; 75
4. Yang, C., Yang, P., Wang, W., Gai, S., Wang, J., Zhang, M., and Lin, J., Synthesis and characterization of Eu-doped hydroxyapatite through a microwave assisted microemulsion process. *Solid State Sci.*, 2009, 11; 1923-1928.
5. Yan, W. Q., Nakamura, T., Kawanabe, K., Nishigochi, S., Oka, M., and Kokubo, T., Apatite layer-coated titanium for use as bone bonding implants. *Biomaterials*, 1997, 18; 1185.
6. Yingguang, L., Zhuoru Y., and Jiang, C., Preparation, characterization and antimicrobial property of cerium substituted hydroxyapatite nano particles. *J. Rare Earths*, 2007, 25; 452.
7. Gopi, D., Ramya, S., Rajeswari, D., Surendiran, M., and Kavitha, L., Development of strontium and magnesium substituted porous hydroxyapatite/poly(3,4-ethylenedioxythiophene) coating on surgical grade stainless steel and its bioactivity on osteoblast cells. *Colloids Surf., B*, 2014, 114; 234-240.
8. Omer Kaygili., Sergey, V., Dorozhkin., and Serhat Keser., Synthesis and characterization of Ce-substituted hydroxyapatite by sol-gel method, *Mater. Sci. Engi. C*, 2014, 42; 78-82.
9. Yousheng, O., Yushan, X., Shaozao, T., and Qingshan, S., Structure, antibacterial activity of Ce<sup>3+</sup> exchanged montmorillonites, *J. Rare Earths* 2009, 27; 858.
10. Feng, Q.L., Kim, T.N., Wu, J., Park, E.S., Kim, J.O., Lim, D.Y., and Cui, F.Z., Antibacterial effects of Ag-HAp thin films on alumina substrates, *Thin Solid Films* 1998, 335; 214.
11. Gopi, D., Collins Arun Prakash, V., Kavitha, L., Kannan, S., Bhalaji, P.R., Shinyjoy, E., and Ferreira, J.M.F., A facile electrodeposition of hydroxyapatite onto borate passivated surgical grade stainless steel. *Corros. Sci.*, 2011, 53; 2328.

\*\*\*\*\*